CHANNEL NORMALIZATION FOR UNSUPERVISED SPECTRAL SUBTRACTION

Guillaume Lathoud [a,b]
Mathew Magimai.-Doss [a,b]
Hervé Bourlard [a,b]

IDIAP–RR 06-09

FEBRUARY 2006

REVISED IN JUNE 2006

[a] IDIAP Research Institute, CH-1920 Martigny, Switzerland
[b] Ecole Polytechnique Fédérale de Lausanne (EPFL), CH-1015 Lausanne, Switzerland

Channel Normalization for Unsupervised Spectral Subtraction

Guillaume Lathoud   Mathew Magimai.-Doss   Hervé Bourlard

Abstract. Application domains such as in-car human-machine interaction require noise-robust front-ends in order to cope with the noisy situations encountered in practice. Moreover, when speech is captured through a cellphone, the phone channel characteristics are often unknown. It is thus desirable to estimate and remove both phone channel characteristics and ambient noise, in an online manner. The main contributions of this paper are twofold. First, a novel channel normalization method is proposed, that is used *before* noise reduction, at the magnitude spectrogram level. It removes the convolutive channel, and reduces the stationary part of the ambient noise. Second, an alternative to classical spectral subtraction is proposed, called "Unsupervised Spectral Subtraction" (USS), which does not require any parameter tuning. Channel normalization followed by USS (two steps) permit to reach an ASR performance very similar to that of the ETSI Advanced Front-End (Wiener filtering, with many steps and parameters). The computational cost of the proposed approach is very low, which makes it fit for real-time applications. Furthermore, channel normalization followed by the ETSI Advanced Front-End leads to a major improvement in noisy conditions, and best overall results.

$$s(t) \longrightarrow \oplus \longrightarrow \boxed{h(t)} \longrightarrow x(t)$$
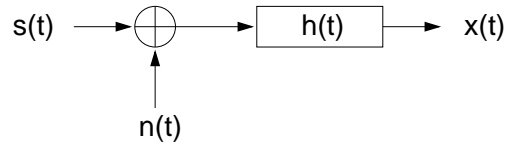
$$n(t)$$

Figure 1: Model of the problem: recognize speech from the observed signal $x(t) = h(t) * (s(t) + n(t))$, where $n(t)$ is the additive acoustic noise and $h(t)$ is the transmission channel (e.g. cellphone).

1 Introduction

Robustness to various noise conditions is a key feature for speech processing algorithms to be turned into versatile, real-world applications. Most often, two exclusive directions are followed: either enhance the speech signal itself by ideally filtering out the noise [1, 2, 3], or change the way acoustic features are extracted from the signal [4, 5]. This paper presents an intermediary approach that enhances the feature extraction process at a level as close as possible to the original signal : at the magnitude spectrogram level, i.e. in time-frequency plane (TF). It relies on a channel normalization step followed by unsupervised EM fitting [6] of a 2-component model on observed data. It can be seen as a parameter-free generalization of classical spectral subtraction methods.

The problem addressed by this paper is Automatic Speech Recognition (ASR) in acoustic noise (e.g. car noise) *followed* by an unkown transmission channel (e.g. cellphone). The goal is to be able to use, in noisy test conditions, HMM models trained on clean data (multi-condition training is not considered in this paper). A possible linear model of the problem is depicted in Fig. 1: to the original speech signal $s(t)$, acoustic noise $n(t)$ is added, and the sum is transmitted over a convolutive channel $h(t)$, thus leading to the following linear model for the received signal $x(t)$:

$$x(t) = h(t) * (s(t) + n(t)) \tag{1}$$

where $*$ denotes the convolution operator. One contribution of this paper addresses estimation and removal of $h(t)$. As a first step, we have implicitly neglected *additive* channel noise in Eq. 1. This is justified by the present focus on noise-robust ASR: it means that $h(t) * (s(t) + n(t))$ is supposed larger than channel noise, at all times. The idea is to validate the proposed channel normalization method first. A more complex model is left for further work.

Classical noise reduction methods such as Wiener filtering, as in the ETSI Advanced Front-End [7], and spectral subtraction methods [8, 9, 10, 11] implicitly assume a flat transmission channel: $h(t) = 1$. One common way to remove the channel is linear post-processing of the MFCC features, *after* noise reduction, such as Cepstral Mean Subtraction (CMS) and Blind Equalization [7]. We argue that non-linearities in the noise reduction stage may prevent CMS and Blind Equalization from completely removing the channel distorsion.

Therefore, this paper considers channel normalization at the signal level, *before* noise reduction and feature extraction (Fig. 2). The main contribution of this paper is to transform the Low-Energy Envelope Tracking (LEET) additive noise estimation method [12, 10] into a channel estimation method. The proposed channel estimation relies on the observation that spectral valleys of the time-frequency plane are dominated by noise. Using spectral valleys, $h(t) * n(t)$ is estimated, and thus $h(t)$, with a white noise assumption. It is then sufficient to divide the received spectrum by the estimated frequency-domain channel response. In practice, for non-white noises, the channel is still normalized, and the stationary part of the additive noise is reduced (divided by a large factor).

Assuming that the transmission channel has been normalized out, the next task is removal of the additive noise $n(t)$. Classical spectral subtraction [8] does it in two steps, in the frequency domain. First, the noise power is estimated in all points of the TF plane, second, it is subtracted from the observed noisy speech power. This relies on a reasonable independence assumption between speech and noise. In our understanding, the main issue of spectral subtraction is the initial noise power
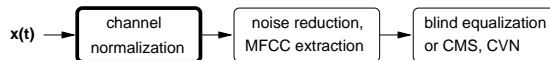
Figure 2: Proposed channel normalization (leftmost block): *before* noise reduction and feature extraction. Note that we still use post-processing (blind equalization or CMS,CVN).

estimate (first step). Ideally, a perfect noise power estimate in all points of the TF plane would require a perfect speech power estimate, which is precisely what we are trying to obtain (second step). Very often, tunable parameters are employed [9] to compensate imperfections such as musical noise. The disadvantage of tunable parameters is that various types of data may lead to different optimal parameter values [9], thus requiring human supervision.

As an alternative to this 2-step approach, the present paper proposes to *jointly* model both distributions of speech and noise magnitudes in the TF plane. The underlying motivation is to rely on the estimated posterior probability of observing speech at a given point of the TF plane. In spirit, the proposed approach is related to TRAP-TANDEM [13] and further developments [14], although the probabilistic modeling is made here at a much lower level: the magnitude spectrogram.

Enhancing the spectrogram itself, based on probabilistic assumptions [15], led to applications to noise-robust ASR [16, 17], and has received much attention recently [2, 3]. In order to build a probabilistic model, at least two distributions are needed: one for background additive noise, and one for speech. A reasonable model for background noise on silent parts of the TF plane is a white Gaussian assumption for real and imaginary parts, which translates into assuming a Rayleigh probability density function (pdf) in the magnitude domain [18]. However, modeling of the speech part is much more complicated, as such an assumption does not hold anymore. Supergaussian models such as the Laplace pdf may be needed [2] for a better fit on real data. Derivation of the magnitude pdf of speech is still an open question [19].

On the contrary, this paper proposes to restrict the problem to modeling of large magnitudes of speech only. Intuitively, low speech magnitudes cannot be distinguished from background noise, being intrinsically regions of low Signal-to-Noise Ratio (SNR). We therefore complete the well-justified background noise Rayleigh model with an ad-hoc pdf for activity, that models "large" magnitudes only. "Large" is defined w.r.t. the Rayleigh model itself, and the complete modeling process is fully unsupervised. We apply this approach to enhance the noise-robustness of single channel ASR by removing noise from the magnitude spectrogram using a modified spectral subtraction. The magnitude spectrogram is filtered at a small cost, so that only speech that can be distinguished from background noise is retained. No parameter tuning is involved, thus justifying the "Unsupervised Spectral Subtraction" designation (USS). It was introduced in [11]. One intent of this paper is to determine whether a type of probabilistic model similar to the one used for microphone array-based speech detection, in [20], can be applied to the context of noise-robust ASR.

Overall, the purpose of this paper is *not* to propose novel noise-robust ASR features, but rather a simple, generic approach that can be a pre-processing step for any acoustic feature extraction process (MFCCs, PLP, etc.). Training on clean data is then sufficient to cope with unseen noise environments. Such an approach is very much in the spirit of [17] and [10]. The two steps of the proposed approach – channel normalization and USS – rely on a consistent model: in both cases, the background noise of the *preemphasized* signal is supposed to be a slowly-varying white Gaussian noise. Although simplistic, it is justified by observations on real data (Fig. 5), and may be deemed the natural first step, before trying more complex noise models.

In experimental studies on the Aurora 2 corpus [21], we first compare the proposed approach with a classical spectral subtraction method [9] selected from the comprehensive study in [10]. The main difference is that the proposed approach – channel normalization followed by USS – does not require any parameter tuning. A clear improvement is obtained in all conditions. Second, we compare the proposed approach with the more complex, many-step ETSI Advanced Front-End [7], which is essentially a two-pass Wiener filter. The results show that channel normalization followed by

USS permits to reach the same performance as that of the ETSI Advanced Front-End. This is quite interesting, given that the proposed signal transformation is fully described by two equations (Eqs. 6 and 18), while the ETSI Advanced Front-End includes many steps and parameters. An initial experiment with channel normalization followed by the ETSI Advanced Front-End shows that further improvement can be obtained in very noisy conditions (0 and 5 dB) for a limited loss at 15 and 20 dB. This suggests further work towards the direction of joint channel/noise estimation. The computational cost of both channel normalization and USS is very small, so that the proposed approach is fit for real-time applications.

The rest of this paper is organized as follows: Section 2 defines notations, Section 3 summarizes existing spectral subtraction methods and identifies three issues with respect to the present task. Section 4 addresses the channel normalization issue. Section 5 addresses the two remaining issues: a probabilistic method for joint speech/noise magnitude estimation is proposed, followed by a parameter-free spectral subtraction procedure. Section 6 presents ASR results on noisy telephone speech [21]. Section 7 concludes the paper. A complete MATLAB implementation of the proposed approach is available at: http://glat.info/ma/2006-CHN-USS/

2   Notations

Both time t and frequency f are discretized into samples and N_{bins} frequency bins (narrowbands), respectively. $x(t)$ or y_t is the pre-emphasized signal, $\mathcal{F}^x_{f,t} \in \mathbb{C}$ is the Discrete Fourier Transform (DFT) of a windowed signal $[x_{t-N_{\text{samples}}+1} \ldots x_t]^{\text{T}}$ (using Hamming window), $[\cdot]^{\text{T}}$ denotes the transposition operator. $m(f,t) = m_{f,t} \stackrel{\text{def}}{=} |\mathcal{F}^x_{f,t}|$ is the magnitude in TF plane, and $w(f,t) = w_{f,t} \stackrel{\text{def}}{=} |\mathcal{F}^x_{f,t}|^2$ the power. x, m and w designate the realizations of random variables X, M and W. The pdf of X is denoted $q_X(x)$. The mathematical expectation of a random variable X is written $\mathbf{E}\{X\} \stackrel{\text{def}}{=} \int_{-\infty}^{\infty} x \cdot q_X(x) \cdot dx$.

3   Classical Spectral Subtraction

This section briefly summarizes the principle of spectral subtraction, and points at open issues in the context of noise-robust ASR that was described in Section 1.

3.1   Principle

For speech enhancement, Boll [8] proposed an additive noise removal procedure called "spectral subtraction". The proposed model is $x(t) = s(t) + n(t)$, where x, s and n designate the received noisy signal, the clean speech signal and the noise signal, respectively. We represent the corresponding time-domain random variables $X(t)$, $S(t)$ and $N(t)$, and assume independence between the clean speech signal $S(t)$ and the noise $N(t)$. The frequency domain power random variable $w_X(f,t)$ then follows:

$$\mathbf{E}\{w_X(f,t)\} \quad = \quad \mathbf{E}\{w_S(f,t)\} \quad + \quad \mathbf{E}\{w_N(f,t)\}, \tag{2}$$

which leads to the following procedure for noise removal:

$$\hat{w}_s(f,t) \quad = \quad \max(0, \quad w_x(f,t) - \hat{w}_n(f,t)), \tag{3}$$

where $\hat{w}_s(f,t)$ and $\hat{w}_n(f,t)$ designate estimated powers of clean speech signal and noise, respectively. Under stationarity and ergodicity assumptions, these estimates can be obtained through DFT over a stationary interval, 20 to 30 ms in the case of speech. Section 3.2 summarizes a method for automatic estimation of $\hat{w}_n(f,t)$.

Berouti [9] considered the issue of musical noise: Eq. 3 introduces many additional zeroes in the TF plane, which in turns make the spectral peaks more narrow. Thus, when reconstructing the

signal $\hat{s}(t)$ from the estimated speech spectrum $\hat{w}_s(f,t)$, this produces an audible "musical noise", which is detrimental to human listening quality, and potentially to ASR. Thus, the following modified procedure was proposed:

- Compute an intermediate estimate $w_d(f,t) = w_x(f,t) - \alpha \cdot \hat{w}_n(f,t)$, where $\alpha \geq 1$ is called the "subtraction factor". The purpose of α is to reduce the amplitude of the remnant noise peaks.

- Estimate the clean speech power as $\hat{w}_s(f,t) = \max(w_d(f,t), \quad \beta \cdot \hat{w}_n(f,t))$, where β is called the "spectral floor parameter" $(0 < \beta << 1)$. β is used to reduce the amplitude of the remnant noise peaks, relatively to the surrounding spectral valleys.

The two steps can be written in a compact manner:

$$\hat{w}_s(f,t) = \max(w_x(f,t) - \alpha \cdot \hat{w}_n(f,t), \quad \beta \cdot \hat{w}_n(f,t)). \tag{4}$$

3.2 Noise Level Estimation (LEET)

In order to apply Eq. 4, it is necessary to first estimate the noise level $\hat{w}_n(f,t)$ at each point (f,t) of the TF plane. This can be done on parts of the TF plane where the speaker is assumed silent, for example obtained with a Voice Activity Detector (VAD). Without VAD, automatic methods can be employed to distinguish between speech harmonics and noise [10]. An extensive study was presented in [10], which essentially compared four different additive noise estimation methods:

- Energy clustering [17]: the distribution of log energies is assumed to present two modes, one for noise, the other for speech (with larger values). The two modes can be fitted with either EM fitting [6] of two Gaussians, or 2-means clustering.

- Hirsch histograms [22]: a histogram of log energies, computed over several hundreds milliseconds, exhibits a peak in the low energy portion. This peak is indicative of the noise level.

- Weighted average [22]: a first-order recursion is used to update the noise estimate, whenever speech is deemed absent.

- Low-Energy Envelope Tracking (LEET) [10], which was derived from [12]. It relies on spectral valleys to estimate a quantity proportional to the noise level.

From this extensive study [10], we selected LEET, as it provided the best results. LEET assumes that low energies – spectral valleys – are dominated by noise. Thus, within each frequency band f, the noise energy is estimated from the average energy of 20 % of the time frames: those with the lowest energy values (Fig. 4).

The LEET noise level estimation assumes that the lowest power values in a portion of the TF plane are essentially dominated by noise. This is a reasonable assumption when noise is more stationary than speech and the global SNR is greater than zero. In particular, it means that the spectral valleys in between speech harmonics mostly contain noise. In practice, LEET is implemented as follows:

- Within a frequency band and a time window, compute the average $\overline{w}_\gamma(f)$ of the 20% lowest power values, denoted by $\gamma = 0.20$. In practice, γ does not require tuning.

- The (locally stationary) noise power is estimated as:

$$\hat{w}_n^{\text{LEET}}(f) \stackrel{\text{def}}{=} C \cdot \overline{w}_\gamma(f), \tag{5}$$

  where $C > 1$ is a correction factor. We used a 5-point $(\approx 150\,\text{Hz window})$ running mean filter in the log power domain $\log(\hat{w}_n^{\text{LEET}}(f))$, across the frequency bins f, in order to eliminate the outliers.
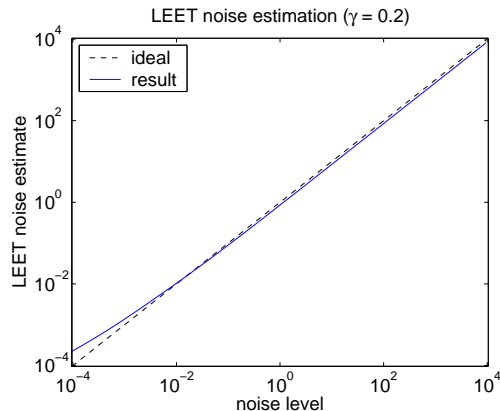
Figure 3: Evaluation of the LEET noise estimation. "Noise level" means the average white gaussian noise energy divided by the average clean speech energy.

In [10], C is SNR-dependent, and is determined by a calibration procedure on training data. In preliminary experiments on OGI Numbers 95 [23], we found that a fixed value $C = (1.5 \gamma)^{-2}$ provides better recognition results than the calibration procedure. Fig. 3 shows an evaluation on clean speech [23] with white noise added at different levels. The slight tilt at the lowest noise levels is due to a very small background noise already present in the "clean" speech signal. Overall, we can see that the noise level estimate is very close to the true noise level.

3.3   Application to Noise-Robust ASR

Following [10], we used Eqs. 4 and 5 to modify the spectrum prior to MFCC extraction of a standard HMM/GMM recognizer. In order to optimize the process for noise-robust ASR, we had to tune the α and β parameters. On the task considered in Section 6.5, we observed best speech recognition results with a constant $\alpha = 2.3$, and $\beta = 0.2$. The spectral floor value $\beta = 0.2$ is much larger than advised in [9]. However, [9] was targetting a speech enhancement task, while the focus here is on MFCC-based ASR. Certain types of speech distorsions may be acceptable for machines, but not for humans, and vice-versa. A high value of the spectral floor is also successfully used in the spectral subtraction variant introduced below (Section 5.3).

Overall, with respect to the noise-robust ASR task and the model depicted in Fig. 1, three issues can be identified.

Issue 1: The model in Section 3.1, $x(t) = s(t) + n(t)$, implicitely assumes a flat transmission channel, i.e. $h(t) = 1$. Thus, the ASR performance may considerably degrade when the channel is *not* flat (e.g. cellphone). It is verified experimentally with LEET on the Aurora 2 task [21], in Section 6.5. In order to fully exploit the potential of spectral subtraction in such environments, the channel response must *first* be estimated and normalized out. Section 4 proposes two methods.

Assuming that the channel $h(t)$ has been normalized out, two general issues remain.

Issue 2: Any error in the noise level estimate $\hat{w}_n(f, t)$ directly impacts on the ASR performance. Based on the additive noise model $x(t) = s(t) + n(t)$, a perfect noise estimation method would require perfect knowledge of the clean signal $s(t)$, which is precisely what we are trying to estimate. This "circular" issue can be addressed by joint modelling of noise and speech, as proposed in Section 5.2.

Issue 3: For each different task, α and β need to be tuned. According to [9], α and β should even vary depending on the local SNR in the TF plane. In our understanding, α and β not only help to reduce musical noise, but also to correct errors in the noise estimation process (especially α). Thus, this issue could be closely related to "Issue 2". Consequently, addressing "Issue 2" could in turn allow

for a simpler, parameter-free spectral subtraction, as proposed in Section 5.3.

4   Channel Estimation and Normalization

Noise reduction methods for ASR include, among others, Wiener filtering, as for example in the ETSI Advanced Front-End [7], and spectral subtraction [8, 9, 10, 24]. They implicitly assume no channel distorsion ($h(t) = 1$), as in the signal model $x(t) = s(t) + n(t)$. In reality, the channel may be distorted, and there may be a mismatch between the channels used in training and test conditions (e.g. different types of cellphones). This mismatch causes a degradation in WER, as the test signals appear distorted to the models trained on data with different channel(s).

In the case of noise-robust ASR, we postulate that channel normalization *after* noise reduction, such as CMS, may not be able to fully remove the channel distorsion, because of non-linearities in the noise reduction process. Following [25, 26], we thus propose to remove the channel *before* any other processing, i.e. at the power spectrum level, as depicted in Fig. 2. The idea is to estimate the power domain channel response $\hat{w}_h(f)$ from the observed signal x, then to remove it through a division in the power domain:

$$w_x^{\text{NORM}}(f,t) \quad = \quad \frac{w_x(f,t)}{\hat{w}_h(f)} \tag{6}$$

The next two subsections propose two different estimates $\hat{w}_h(f)$, corresponding to two different sets of assumptions. The main contribution of this paper lies in the second one (CHN).

4.1   Geometric Mean Normalization (GMN)

We propose here to use existing dereverberation methods [25, 26] to do channel normalization. These existing methods consist in removing the mean in the log power domain.

Let us examine which assumption lies behind such a normalization. First, the time-domain signal model of Eq. 1 can be translated to the log power domain:

$$\log w_x(f,t) \quad = \quad \log w_h(f) + \log(w_{s+n}(f,t)) \tag{7}$$

We now assume that:

$$\langle \log(w_{s+n}(f,t)) \rangle_t \quad \approx \quad L \tag{8}$$

where $\langle \cdot \rangle_t$ denotes the mean across DFT time frames, and L is a constant: it does not depend on frequency f. This assumption is partly justified by the pre-emphasis done in the time domain, which flattens the spectrum. Then, $\log w_h(f) \approx \langle \log w_x(f,t) \rangle_t - L$, which justifies to divide the observed power values $w_x(f,t)$ by their geometric mean, within each frequency band f:

$$\hat{w}_h^{\text{GMN}}(f) \quad \overset{\text{def}}{=} \quad \exp \langle \log w_x(f,t) \rangle_t \tag{9}$$

One could object that on "short" speech signals, as typically encountered in hands-free dialing of a telephone, the assumption $L(f) = \text{const}$ is not justified. Indeed, $L(f)$ would most likely reflect the speaker-specific harmonics, and thus depend on f.

4.2   Proposed CHannel Normalization (CHN)

As an alternative to GMN, we propose to use a different assumption, in order to turn any additive noise estimation method into a channel estimation process. Assuming independence between speech $s(t)$ and noise $n(t)$, the time-domain signal model of Eq. 1 becomes a product in the frequency domain:

$$\begin{aligned} w_x(f) \quad &= \quad w_h(f) \cdot (w_s(f) + w_n(f)) \\ &= \quad w_h(f) \cdot w_s(f) + w_h(f) \cdot w_n(f) \end{aligned} \tag{10}$$
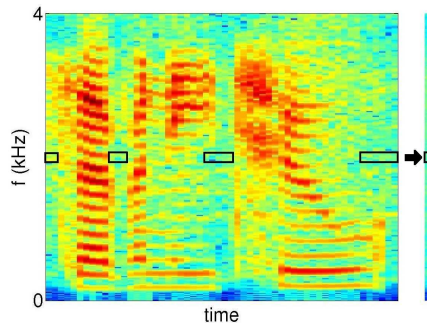
Figure 4: Estimation from the lowest energies within each band (LEET and CHN).

Applying an additive noise estimation method in such a case would lead to estimate the second term on the right-hand side, i.e. the distorted noise $w_h(f) \cdot w_n(f)$. Making a simplified white noise assumption $w_n(f) = \text{const}$, it follows that $w_h(f) \cdot w_n(f)$ is directly proportional to the channel gain $w_h(f)$. The "additive noise estimate" can thus be used as the denominator $\hat{w}_h(f)$ in Eq. 6.

Following the independence and white noise assumptions mentioned above, we propose to turn the LEET noise estimation method (Section 3.2) into a channel estimation method. The channel gain $\hat{w}_h(f)$ is estimated within each frequency band f, using the geometric mean of the lowest power values (Fig. 4). Formally, for each frequency band f:

$$\hat{w}_h^{\text{CHN}}(f) \quad \overset{\text{def}}{=} \quad \exp\left[\; \langle\, \log w_x(f,t)\, \rangle_{w_x(f,t) < K_\gamma(f)} \;\right] \tag{11}$$

where $K_\gamma(f)$ is the $(100 \cdot \gamma)^{\text{th}}$ percentile of observed power values $w_x(f,t)$ within a time window. Typically $\gamma = 0.20$, as in the LEET method [10]. We did not consider tuning of γ: the value used here is exactly the same as in [10].

A 5-point running mean across frequencies ($\approx 150\,\text{Hz}$ window) is then applied in the log power domain $\log \hat{w}_h(f)$ to remove outliers. Note that the use of geometric mean (Eq. 11) makes the normalization procedure (Eq. 6) independent of the chosen representation (magnitude $m(f,t)$ or power $w(f,t)$). While the additive noise estimation is standard, to the best of our knowledge, the proposed approach for channel normalization is novel.

In practice, the white noise assumption is not verified. In such cases, not only the estimated channel gain is normalized out, but also the stationary part of the additive noise is largely reduced (divided by a large factor). This is confirmed by the ASR results in Section 6.5. The choice for a simplistic white noise assumption is deliberate: the goal is to assess *experimentally* whether or not channel normalization *before* non-linear noise reduction can be beneficial or not. Experiments reported in Section 6.4 confirm the idea.

On the implementation side, note that clean telephone speech contains some time frames with a null signal, due to built-in speech/silence detectors. In such a case $s(t) + n(t) = 0$, so the channel estimate is not updated, and the null signal is left as is.

5   Unsupervised Spectral Subtraction

This section addresses the second and third issues mentionned in Section 3.3: noise level estimation and parameter-free spectral subtraction. The focus is *not* speech enhancement for human listening, but rather noise-robust ASR.

In Sections 5.1 and 5.2, the commonly used Rayleigh silence model is justified on real data, and completed with an ad-hoc speech activity model. The main difference with existing, related models
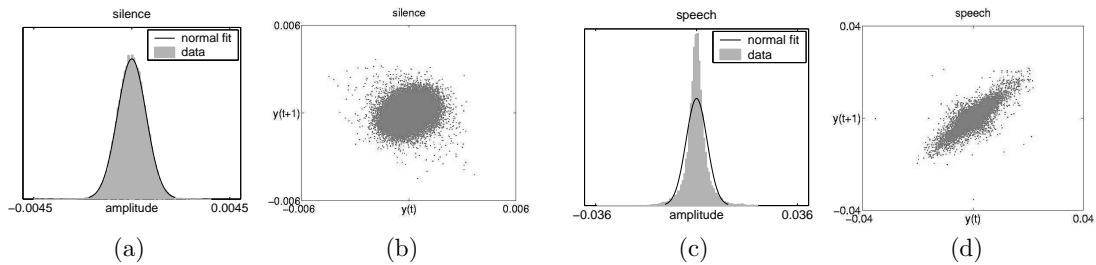
Figure 5: Observations on real meeting room data [27] (pre-emphasized waveform $x(t)$). (a),(c): histograms, (b),(d): phase plots.

such as in [15, 2, 3], is that we do not address the complete probabilistic modeling of speech activity, but limit ourselves to large magnitudes only.

Based on this model, Section 5.3 proposes a parameter-free alternatives to the classical spectral subtraction procedure described in Section 3.

5.1 Observations on Real Waveforms

Simple observations on silence periods of a pre-emphasized waveform $x(t)$ and its covariance matrix, as partially illustrated by Figs. 5a and 5b, show that modeling $X(t)$ as a i.i.d, zero-centered Gaussian process is very reasonable. From this assumption, the real and imaginary part of the DFT are independent Gaussian distributed variables, as shown in Appendix A. (An exact derivation is given, without asymptotical considerations such as the central limit theorem). Thus, on silent parts of the TF plane, the magnitude $M_{f,t}$ has a Rayleigh pdf [18]. This type of assumption is used in [2, 19]. It is consistent with the white noise assumption that is used in the proposed channel normalization method (Section 4.2). In practice, as described below, we process the signal in 1-second blocks, thus permitting the white Gaussian noise level to be slowly time-varying.

On the other hand, speech waveforms are clearly *not* Gaussian distributed, and *not* i.i.d., as shown by Figs. 5c and 5d. As mentioned in Section 1, finding a fully-justified pdf for speech magnitude is still an open question [19]. Thus, the next section proposes to only model large magnitudes of speech.

5.2 Proposed 2-Component Mixture Model (RSE)

The proposed pdf for the magnitude random variable M is $q(m) \stackrel{\text{def}}{=} P_{\text{I}} \cdot q_{\text{I}}(m) + P_{\text{A}} \cdot q_{\text{A}}(m)$, where P_{I} and P_{A} are the priors for "silence" and "speech activity", respectively. Note that the model is independent of f and t.

q_{I} is the Rayleigh pdf:

$$q_{\text{I}}(m) \quad \stackrel{\text{def}}{=} \quad \frac{m}{\sigma_{\text{I}}^2} \ e^{-\frac{m^2}{2\sigma_{\text{I}}^2}}, \tag{12}$$

and q_{A} is a pdf that models magnitudes $m > \delta_{\text{A}}$, where δ_{A} is a threshold defined w.r.t. q_{I}. As a starting point, in this paper we use $\delta_{\text{A}} = \sigma_{\text{I}}$, which is the mode of the Rayleigh pdf. The reasoning is that values below the mode of the Rayleigh q_{I} can safely be assumed to be background noise.

Moreover, we constrain q_{A} to fulfill two practical constraints. First, the derivative $q'_{\text{A}}(m)$ of the chosen "speech activity" pdf should not be zero when m is just above δ_{A}, otherwise the threshold δ_{A} will loose its meaning, as it may be set to an arbitrarily low value. Second, the decay of $q_{\text{A}}(m)$ when m tends towards infinity should always be lower than the decay of the Rayleigh. This ensures that f_{A} will capture data with large magnitudes, and not f_{I}. A pdf that fulfills the two criterions above is

a "shifted Erlang" pdf with h=2 (the Erlang pdf belongs to the Gamma family [18]):

$$q_A(m) \quad \overset{\text{def}}{=} \quad \mathbf{1}_{m>\sigma_I} \cdot \lambda_A^2 \cdot (m - \sigma_I) \cdot e^{-\lambda_A(m-\sigma_I)}, \tag{13}$$

where $\mathbf{1}_{m>\sigma_I}$ is equal to 1 if $m > \sigma_I$, and zero otherwise. Note the implicit stationarity assumption: the 4 parameters $\Lambda = \{P_I, \sigma_I, P_A, \lambda_A\}$ are assumed to be independent of t. Furthermore, independence of f is also assumed; it is partially justified by the pre-emphasis, which whitens the spectrum. The RSE model is similar to the probabilistic model used for microphone array-based speech detection, in [20].

EM training of Λ: The proposed mixture model can be trained using the EM algorithm [6]. Both "E" and "M" steps involve simple mathematical expressions. In the "E" step, posteriors can be estimated as follows:

$$P(\text{sil}|m_{f,t}, \Lambda) \quad = \quad \frac{P_I \cdot q_I(m_{f,t})}{P_I \cdot q_I(m_{f,t}) + P_A \cdot q_A(m_{f,t})} \tag{14}$$

$$P(\text{act}|m_{f,t}, \Lambda) \quad = \quad 1 - P(\text{sil}|m_{f,t}, \Lambda) \tag{15}$$

In the "M" step, exact maximization of the likelihood is difficult: since parameters σ_I and λ_A are tied in a non-linear fashion (Eq. 13), we have not found a way to separate them analytically. From this constatation, we propose two options:

1. Numerical optimization of the exact likelihood of the observed data through simplex search in the (σ_I, λ_A) space (e.g. `fminsearch` in MATLAB). In this case, the M step requires several sub-iterations before reaching a local maximum. We refer to this option as "**ML**".

2. Analytical approximation through a moment-method, in a single step. First σ_I is updated using all data, then λ_A is updated using all data with values above the new σ_I value. This option is referred to as "**moment**". It is defined by the following update equations:

$$\hat{\sigma}_I \quad = \quad \left[\frac{\sum\limits_{f,t} m_{f,t}^2 \cdot P(\text{sil}|m_{f,t}, \Lambda)}{2 \sum\limits_{f,t} P(\text{sil}|m_{f,t}, \Lambda)} \right]^{\frac{1}{2}} \tag{16}$$

$$\hat{\lambda}_A \quad = \quad \frac{\sum\limits_{m_{f,t}>\hat{\sigma}_I} (m_{f,t} - \hat{\sigma}_I)^{-1} \cdot P(\text{act}|m_{f,t}, \Lambda)}{\sum\limits_{m_{f,t}>\hat{\sigma}_I} P(\text{act}|m_{f,t}, \Lambda)} \tag{17}$$

Data representation: As opposed to histogram-based implementations, in this paper the cost is reduced, using a direct representation with a reduced set of samples (no weights). In all results reported in this paper, only 100 representative samples are used: observed magnitude values are sorted in an increasing manner, from which 100 samples are picked at regular intervals. This data reduction method is equivalent to estimate percentile values at equal steps.

Figs. 6a, 6b and 6c show an example of fit on one file taken from the OGI Numbers 95 database [23]. (OGI Numbers 95 is used because its transmission channel is flat.) In the following, we'll refer to the Rayleigh and Shifted Erlang model as "RSE".

Approximation: it is possible to approximate the σ_I parameter for an even lower computational cost than RSE fitting, as described in Appendix B. The cost is a slight but systematic degradation of the ASR performance.

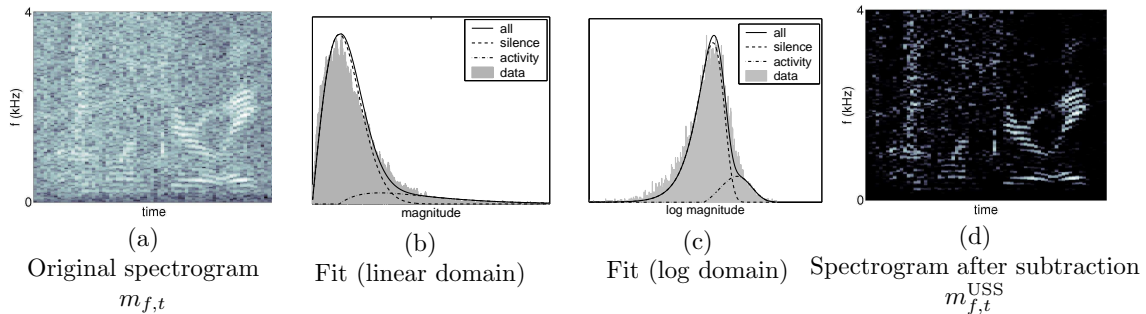| (a) | (b) | (c) | (d) |
| Original spectrogram $m_{f,t}$ | Fit (linear domain) | Fit (log domain) | Spectrogram after subtraction $m_{f,t}^{\mathrm{USS}}$ |

Figure 6: Example of fit of the 2-component model on noisy data taken from the OGI Numbers 95 database (Factory 0dB condition). All plots show magnitude data in the frequency domain. On spectrogram plots (a) and (d), the largest magnitudes are white, the smallest magnitudes are black. (OGI Numbers 95 [23] is used for this example because the transmission channel is flat.)

5.3   USS with the RSE Model (RSE-USS)

A 2-step approach is used:

1. Joint speech/noise modeling with EM fitting of the RSE parameters Λ, as described in Section 5.2, using either "ML" or "moment". Prior ASR studies [11] on OGI Numbers 95 show that "moment" yields better results than "ML". Thus, all RSE-USS results reported below were obtained using "moment".

2. Spectral subtraction using parameter σ_{I} as a floor:

$$m_{f,t}^{\mathrm{USS}} \quad \overset{\text{def}}{=} \quad \max\left(1, \frac{m_{f,t}}{\sigma_{\mathrm{I}}}\right). \tag{18}$$

Note that the flooring to a non-zero value ($\max(1,\dots)$) is necessary in the MFCC context. Indeed, leaving zero magnitude values after spectral subtraction would lead to undesirable dynamics in cepstral coefficients. An example of result of Eq. 18 is shown in Fig. 6d. Although Eq. 18 is not, strictly speaking, the spectral subtraction scheme described by Eq. 4, it has the same two characteristic: noise removal and flooring. We prefered the normalization scheme of Eq. 18 in order to avoid tunable parameters (Issue 3 in Section 3.3). The overall computational cost of RSE-USS (Eq. 18) is small, because posteriors (Eqs. 14 and 15) don't need to be computed. RSE-USS only requires σ_{I}, which can also be obtained for a small cost, as explained in Section 5.2. This justifies the "unsupervised" qualification.

This approach can be compared to previous works. We can note common points "in spirit" with [17] (and to a lesser extent [16]): adaptation to non-stationary noises is possible in both [17] and our approach through block-wise processing, as illustrated by experiments on OGI Numbers 95 reported in [11]. Moreover, on the modeling side, parameters of the "noise" distribution (i.e. silence) are more important than those of the "speech" distribution (i.e. activity) in both approaches, as they are used to floor the magnitude values (max operator).

However, here the modeling is made directly at the magnitude spectrogram level, with a single model for all frequencies, while in [17] modeling was made after mel filterbank computation, and a model was defined for each critical band separately. Furthermore, the approach proposed here is one-pass, fully unsupervised, without any "feedback" loop, without any tunable threshold, without histogram. In [17], multiple stages are involved, including histograms, band-specific parameters, short-term and long-term adaptation, a "feedback" loop, tunable parameters that have to be trained and (optionally) an artificial white noise is injected.

Finally, it is important to realize that in log the domain, the Rayleigh distribution has a fixed shape. Indeed, a change of the σ_{I} parameter only corresponds to a translation in the log-domain,

as proven by the next section. From this perspective, the Rayleigh is a lot more constrained than a log-normal distribution, for example. Although this could look like a disadvantage, it avoids capturing too much speech information with the noise distribution. Thus, with the RSE model, potentially more speech information is conserved in noisy situations.

6 Application to Noise-Robust ASR

This section compares various noise reduction techniques, used as a front-end for an HMM/GMM speech recognizer, on the Aurora 2 task [21]. First, the baseline ETSI Mel-Cepstrum Front-End is presented [28]. Second, the ETSI Advanced Front-End for noise-robust ASR is described [7]. Third, it is proposed to replace the noise reduction part of the ETSI Front-End with a simpler, parameter-free alternative: channel normalization (Section 4.2) followed by USS (Section 5). Results show that the robustness to noise is greatly improved.

6.1 ETSI Mel-Cepstrum Front-End (MFCC)

The ETSI Mel-Cepstrum Front-End [28] is used as a baseline. The output feature vector has 14 components only: log energy and MFCC coefficients C_0 to C_{12} (no derivatives). Normalization techniques such as Blind Equalization or CMS/CVN are not used. In order to have a fair comparison with the noise-robust front-ends described in the following, Voice Activity Detection (VAD) was simulated using "end-pointing". Using the known beginning and end of each speech utterance, all silences before and after were replaced with a fixed 200 ms duration. Results are provided courtesy of Prof. Günther Hirsch and Mr. David Pearce. In the following, we denote this front-end MFCC.

6.2 ETSI Advanced Front-End (AFE)

The ETSI Advanced Front-End for noise-robust ASR [7] includes a sequence of 3 successive parts: (1) noise reduction with double Wiener filtering, (2) MFCC extraction and (3) Voice Activity Detection (VAD).

The first part, noise reduction (depicted in Fig. 7), is expected to remove most of the noise from the time-domain waveform, and output a "denoised" time-domain waveform. It includes a two-pass Wiener filtering, which itself requires SNR estimation in the frequency domain. In the first pass, a specialized detector is applied to separate the speech time frames from the noise time frames. From speech/noise decisions and the observed spectrum, the SNR is estimated at each point of the TF plane, and a Wiener filter is designed in the mel filter-bank domain. The Wiener filter is then applied to the input waveform and a denoised time-domain signal is reconstructed. On this denoised signal, the entire process is repeated a second time, in order to produce an even cleaner signal. Finally, a Teager operator is applied, that emphasizes the high-SNR parts of the waveform. Overall, this first part includes many numerical parameters and "if/then" rules.

In the second part, the "denoised" time-domain waveform is fed into a MFCC extractor. It is essentially standard, with some additional optimizations such as 0.9 pre-emphasis, combination of log energy and C0, and blind equalization.

The third part is optional. It is a sophisticated VAD that combines three different types of measures (mel-warped Wiener filter coefficients, spectral sub-bands and spectral variance). The output is a speech/silence binary decision for each time frame. It can be used to ignore non-speech frames, which aims at improving the ASR performance [7].

In the following, we denote this front-end AFE.

6.3 Proposed Front-Ends

The experimental investigation aims at simplifying the first part of the AFE, noise reduction, replacing the many rules and parameters with simpler approaches. The other two parts of the AFE (MFCC
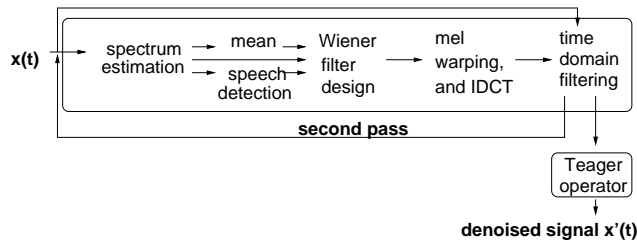
Figure 7: Noise reduction stage of the ETSI front-end.
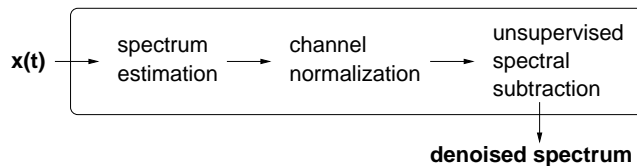

Figure 8: Proposed frequency-domain noise reduction.

extraction and VAD) are kept exactly the same.

For noise reduction, we thus propose a 2-step approach, entirely in the frequency domain (depicted in Fig. 8):

- Channel Normalization: GMN or CHN, described in Sections 4.1 and 4.2.

- Spectral Subtraction: LEET or USS, described in Sections 3 and 5.3, respectively.

In all cases, channel normalization and spectral subtraction are applied in a blockwise fashion (e.g. 1-second blocks) in order to accomodate time-varying background noises. In each frequency band, magnitude observations are accumulated and reduced as described in Section 5.2, for a very small cost. This is similar to a 0.5 forgetting factor, which was already noted to be useful in [17].

Finally, we also test CHN followed by the AFE. Prior normalization (GMN or CHN) must be done by filtering the time-domain signal. The time-domain filter $h(t)$ is estimated through inverse DFT of $\sqrt{\hat{w}_h(f)}$ (Eqs. 9 or 11), half-window delay and Blackman windowing. Note that in the case of the AFE, the Blind Equalization is used as post-processing [7] (as opposed to the CMS/CVN used for LEET and USS.)

6.4   Experiments on Aurora 2

The Aurora 2 task was designed to evaluate the front-end of ASR systems in noisy conditions [21]. The task is speaker-independent connected digit recognition. The database comprises isolated digits and sequences of up to 7 digits from the TIDigits database [29] spoken by male and female US-American adults. The original 20kHz data was downsampled to 8 kHz, in order to obtain a telephone bandpass between 0 and 4 kHz. The resulting data constitutes the clean speech data (clean condition). Noises were then added artificially at different SNR levels (20 dB to -5 dB). The noises were recorded at different places: suburban train (A1), crowd of people (babble) (A2), car (A3), exhibition hall (A4), restaurant (B1), street (B2), airport (B3), and train station (B4). Some noises are fairly stationary, for instance car noise and exhibition noise. Others contain non-stationary segments, as in street noise, babble noise and airport noise.

Finally, as described in [21], two types of transmission channels are considered: flat (test sets A and B) and non-flat (test set C). "Non-flat" means that the frequency-domain response $w_h(f)$ of

the transmission channel has a non-zero slope. It corresponds to some types of GSM cellphones. In the "non-flat" case, the proposed channel normalization presented in Section 4.2 is expected to compensate for the "flat" channel implicitly assumed by spectral subtraction methods. Ideally, the result of a recognizer should be independent of the transmission channel.

The Aurora 2 task defines two different training modes: training on clean condition only, and training on both clean and noisy conditions. In this paper, only experiments with training on clean condition are reported, because the purpose of our approach is precisely to remove noise as much as possible in order to make acoustic modeling as noise-robust as possible, while retaining similar performance in clean conditions. The details about the training set, test set and HTK recognizer can be found in [21].

Based on initial tests [11] done on the OGI Numbers 95 task [23] we selected a 1-second block size and applied the various approaches to the Aurora 2 corpus [21]. The frame shift is 10 ms and the frame length is 25 ms. For all proposed front-ends (except the baseline) 13 MFCC coefficients are extracted (C_0 to C_{12}), along with deltas and delta-deltas, and fed into the Aurora 2 HMM/GMM recognizer [21]. In order to have a fair comparison, for all front-ends (except for the MFCC baseline), the same AFE MFCC/delta/delta-delta extractor and AFE VAD are used [7]. They are briefly described in Section 6.2. As already mentioned, post-processing is done through Blind Equalization in the case of the AFE [7]. On the other hand, post-processing is done with CMS, CVN in the case of spectral subtraction (LEET and USS).

6.5   Results and Discussion

Overall average WER results for each test set A,B,C are presented in Table 1. Averages per noise type are shown in Fig. 9a. Averages per SNR level are depicted in Figs. 9b, 10a and 10b.

In all cases, results on Test Set C (mismatched channel) confirm that normalizing the channel *before* the non-linear noise reduction stage is beneficial, as compared to methods that attempt to normalize the channel *only after* the noise reduction stage (LEET and USS with CMS/CVN, AFE with Blind Equalization). As a by-product, improvement also appears for the other cases (Test Sets A and B), except for the AFE on Test Set A. This is mainly due to the Exhibition noise (A4 in Fig. 9a). In all cases, the proposed channel normalization (CHN) is superior to the existing normalization method (GMN).

The improvement from USS to CHN-USS is quite remarkable, leading to results comparable to those of the AFE: 13.4 % overall average WER for CHN-USS, 13.2 % for the AFE. This is interesting, given that Eqs. 6 and 18 fully describe the modifications of the spectrum. On the contrary, the AFE includes many more rules and parameters [7]. USS also provides results superior to those of LEET, as visible in Table 1. A possible explanation is that LEET was originally designed for speech enhancement for human listening: noise-robust ASR with a HMM/GMM system may have different needs.

The CHN-AFE result has the best overall WER (12.5 %). Compared to AFE (Fig. 10), CHN-AFE yields an improvement in noisy conditions below 10 dB of up to 5 % absolute WER, for a slight degradation above 10 dB (up to 1 % absolute WER), and similar results in clean conditions (0.2 % absolute degradation, the relative variations are not significant). In terms of test sets, there is a degradation on test set A, for an improvement on test sets B and C. In order to assess the cause of the degradation on test set A, we looked at average results for each noise type (Fig. 9a). It appears that the "Exhibition Hall" condition is the main source of problems. From the long-term spectral shapes shown in [21], this noise seems to occupy the largest bandwidth, having a roughly equally-distributed spectrum across frequencies. So it would seem to fit well the white noise assumed by CHN (Section 4.2), which is a contradiction with the degradation observed. One possible explanation is that "Exhibition Hall" also often includes non-white noises, such as people speaking, whistling and some strong voices. This suggests refining the noise model, possibly by doing channel normalization and noise removal jointly. Integrating CHN *inside* the 2-stage AFE process is a possibility.

To conclude, two main observations can be made. First, the proposed "channel normalization" method alone greatly reduces not only the sensitivity to channel variability, but also the stationary

Method	Post-processing	Without VAD				With VAD			
		A	B	C	Ave.	A	B	C	Ave.
MFCC	End-pointing	–	–	–	–	42.6	47.6	37.4	42.5
LEET	CMS,CVN	29.0	27.1	29.4	28.5	27.5	26.0	27.5	27.0
CHN-LEET	CMS,CVN	**26.5**	**24.2**	**27.3**	**26.0**	**24.9**	**22.8**	**25.3**	**24.3**
USS	CMS,CVN	16.9	15.7	20.7	17.8	16.7	15.2	20.5	17.5
GMN-USS	CMS,CVN	14.6	13.1	14.3	14.0	**14.4**	**12.5**	14.3	**13.7**
CHN-USS	CMS,CVN	**14.1**	**12.7**	**13.5**	**13.4**	14.5	12.9	**13.9**	**13.7**
AFE	Blind eq.	**12.3**	12.9	14.6	13.2	**12.5**	12.9	14.4	13.3
GMN-AFE	Blind eq.	14.0	12.2	13.0	13.1	14.3	12.3	13.2	13.3
CHN-AFE	Blind eq.	13.7	**11.5**	**12.2**	**12.5**	14.1	**11.5**	**12.1**	**12.6**

Table 1: Average WER results on Aurora 2. For each test set (A,B,C), the average WER is computed over 0,5,10,15,20 dB conditions. Training is done on clean signals. "Blind eq." and "CMS,CVN" indicate the type of post-processing that was used (rightmost block in Fig. 2). "MFCC" means ETSI Mel-Cepstrum Front-End [28] (MFCC results courtesy of Prof. Günther Hirsch and Mr. David Pearce). "AFE" means ETSI Advanced Front-End [7].

SNR	-5	0	5	10	15	20	clean
MFCC	91.6	85.2	65.6	38.6	17.2	6.1	0.9
USS	77.5	49.3	23.1	9.9	4.2	2.2	**0.9**
CHN-USS	**70.0**	**38.2**	**16.2**	**7.1**	**3.5**	**2.1**	1.1
AFE	69.9	38.1	15.8	**7.0**	**3.4**	**1.9**	**0.8**
CHN-AFE	**66.2**	**33.2**	**14.5**	7.3	4.4	2.9	0.9

Table 2: WER results on Aurora 2, per SNR level, averaged on the 12 noise types A1 to A4, B1 to B4, C1, C2. Training is done on clean signals. Post-processing: as in Table 1.
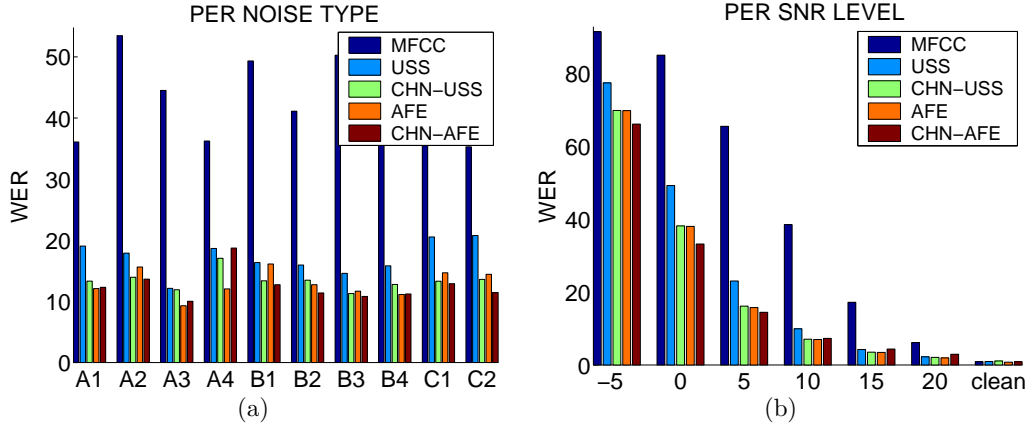

Figure 9: WER results on Aurora 2 (a) for each noise type, averaged on 0, 5, 10, 15, 20 dB SNR levels. A1:Subway, A2:Babble, A3:Car, A4:Exhibition, B1:Restaurant, B2:Street, B3:Airport, B4:Train-station, C1:Subway, C2:Street. (b) for each noise level, averaged across noise types. Training is done on clean signals.
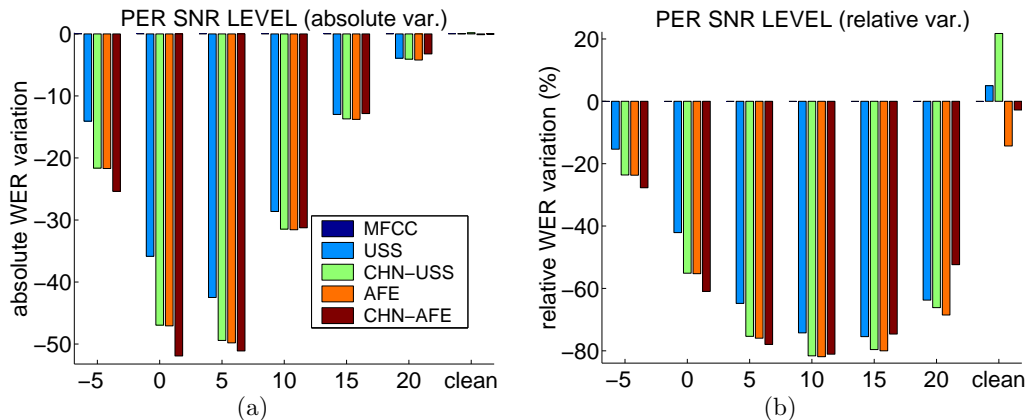
Figure 10: Absolute and relative WER variation (the lower, the better) compared to the ETSI Mel-Cepstrum Front-End (denoted MFCC), on Aurora 2, for all three test sets A, B and C (average). Training is done on clean signals.

part of the additive noise. This is expected due to the non-white nature of real noises, as explained in Section 4.2. Second, the AFE was greatly simplified, by replacing the many-step two-pass Wiener filtering with direct, simple spectral subtraction approaches. Each step of the proposed approach (CHN and USS), relies on a single equation (Eqs. 6 and 18, respectively), and no tuning parameter. CHN-USS yields an ASR performance very similar to that of the AFE, and CHN-AFE yields the best average results. Further improvement may be obtained on clean conditions through expliciting the *additive* channel noise – we neglected it as a first step, focussing on very noisy conditions.

7 Conclusion

Three limitations of classical spectral subtraction were addressed by this paper, in the context of noise-robust ASR. First, a channel normalization method was proposed, in order to extend spectral subtraction to non-flat transmission channels such as cellphones. In practice, the proposed channel normalization method not only removes the convolutive noise due to the channel, but also part of the additive acoustic noise. Results on the Aurora 2 task show that the proposed channel normalization effectively accomodates mismatch channels, and leads to better ASR performance for all front-ends (ETSI Advanced Front-End, as well as spectral subtraction). In particular, the improvement is clear, as compared to methods that attempt to normalize the channel *only after* the non-linear noise-reduction stage. A second limitation addressed by this paper is that the underlying noise estimate is a crucial factor for the ASR performance of spectral subtraction methods. This issue was then postulated to be tightly linked with the third limitation, i.e. the need of task-dependent, condition-dependent tuning factors. As an alternative, a straightforward procedure called "Unsupervised Spectral Subtraction" was proposed, that jointly models speech and noise at the magnitude spectrogram level. It is completely unsupervised, as it does not have any tuning factor. Combined with channel normalization, it provides very similar ASR performance to that of the ETSI Advanced Front-End, on the Aurora 2 corpus. This is quite interesting, given that the proposed signal transformation is fully described by two equations (Eqs. 6 and 18), while the ETSI Advanced Front-End includes many steps and parameters. The absence of tuning factors, and the very low computational cost makes it directly fit for real-time applications on low-power nodes such as cellphones and PDAs. Future work may include several directions. The result with channel normalization followed by the ETSI Advanced Front-End suggests possibilities for further improvement in noisy conditions, for example through

joint noise/channel modelling. This would permit to use more complex noise models than the slowly-varying white Gaussian noise assumption consistently used here. Moreover, improvement in clean conditions may be expected by expliciting the *additive* channel noise term in the signal model.

Acknowledgments

A   Proof of the Rayleigh distribution of magnitudes

In this section we derive the Rayleigh magnitude-domain silence model of $|\mathcal{F}_f^X|$ (Eq. 12), from a white Gaussian assumption for the pre-emphasized signal X_t.

First, let us recall a result originally shown by Rice in 1944 (for a demonstration see [18, pp. 296-297]). Rice showed that given two zero-mean Gaussian, uncorrelated random variables A and B with same standard deviation σ, and $R \stackrel{\text{def}}{=} |A + jB|$, the R variable has a Rayleigh pdf:

$$q_R(r) = \frac{r}{\sigma} e^{-\frac{r^2}{2\sigma^2}} \quad \text{for} \quad r > 0. \tag{19}$$

Let us now define $X_{1:N}$, as a vector of N uncorrelated[1] zero-mean Gaussian random variables $X_{1:N} \stackrel{\text{def}}{=} [X_1 \dots X_N]^{\mathrm{T}}$. The Discrete Fourier Transform (DFT) of X is $\mathcal{F}_{1:N_{\text{bins}}}^X = \left[\mathcal{F}_1^X \cdots \mathcal{F}_{N_{\text{bins}}}^X\right]^T$ where for a given $f = 1 \dots N_{\text{bins}}$:

$$\mathcal{F}_f^X \stackrel{\text{def}}{=} \sum_{n=1}^{N} X_n e^{-2\pi(f-1)\frac{n-1}{N}}. \tag{20}$$

Let $A_f = \mathcal{R}e\left(\mathcal{F}_f^X\right)$ and $B_f = \mathcal{I}m\left(\mathcal{F}_f^X\right)$. In other terms:

$$\begin{cases} A_f = \sum_{n=1}^{N} X_n \cos\left(-2\pi(f-1)\frac{n-1}{N}\right), \\ B_f = \sum_{n=1}^{N} X_n \sin\left(-2\pi(f-1)\frac{n-1}{N}\right) \end{cases} \tag{21}$$

For $f = 1$ we have $A_1 = \sum_{n=1}^{N} X_n$ and $B_1 = 0$.

For $f > 1$: the random variable A_f (resp. B_f) is a weighted sum of zero-mean, single Gaussian random variables, therefore [30, p. 99] it is also a zero-mean, single Gaussian random variable with variance:

$$\begin{cases} \sigma_{A_f}^2 = \sigma^2 \sum_{n=1}^{N} \cos^2\left(2\pi\left(f-1\right)\frac{n-1}{N}\right), \\ \sigma_{B_f}^2 = \sigma^2 \sum_{n=1}^{N} \sin^2\left(2\pi\left(f-1\right)\frac{n-1}{N}\right). \end{cases} \tag{22}$$

Given that $\cos^2 t = \frac{1}{2}(1 + \cos 2t)$ and $\sin^2 t = \frac{1}{2}(1 - \cos 2t)$ we can write:

$$\begin{cases} \sigma_{A_f}^2 = \frac{\sigma^2}{2}\left(N + \sum_{n=1}^{N} \cos\left(4\pi\left(f-1\right)\frac{n-1}{N}\right)\right), \\ \sigma_{B_f}^2 = \frac{\sigma^2}{2}\left(N - \sum_{n=1}^{N} \cos\left(4\pi\left(f-1\right)\frac{n-1}{N}\right)\right). \end{cases} \tag{23}$$

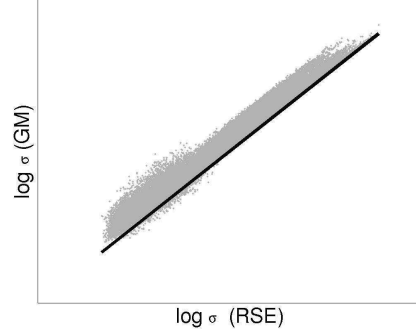[1]Uncorrelation and independence are equivalent for Gaussian random variables.

Figure 11: Comparison between the σ parameter estimated by fitting a RSE model (Section 5.2) and the geometric mean of *all* observed magnitude values (Section B). The graph is shown in the log domain (grey points), and the dark line represents equality. In the linear domain, the correlation is 0.97 and the slope is 1.26.

Let us now write the complex domain sum:

$$\sum_{n=1}^{N} e^{j4\pi(f-1)\frac{n-1}{N}} \;=\; \sum_{n=0}^{N-1} \alpha^n \;=\; \frac{1-\alpha^N}{1-\alpha} = 0, \tag{24}$$

because $\alpha^N = 1$, where $\alpha = e^{j4\pi\frac{f-1}{N}}$. (Since $1 < f \leq N$, $\alpha \neq 1$ and all terms in Eq. 24 are defined.) From Eq. 23, and the real part of Eq. 24, we conclude that:

$$\sigma_{A_f} = \sigma_{B_f} = \sigma\sqrt{\frac{N}{2}}. \tag{25}$$

Similarly, the cross-correlation $\sigma_{A_f B_f} \stackrel{\text{def}}{=} \mathbf{E}\{A_f B_f\}$ can be shown to be zero, using the imaginary part of Eq. 24 and the uncorrelation hypothesis on the X_n variables.

To conclude, we have shown that the random variables A_f and B_f are zero-mean, uncorrelated single Gaussian random variables of same variance, therefore the result of Rice applies:

For $f > 1$, $\left|\mathcal{F}_f^X\right|$ has a Rayleigh pdf of parameter $\sigma\sqrt{\frac{N}{2}}$.

B   Simplified Geometric Mean Noise Estimation of the RSE

The estimated parameter $\hat{\sigma}_{\text{I}}$ of the RSE model (Section 5.2) is shown here to be closely related to the geometric mean of a Rayleigh distribution. We assume a Rayleigh-distributed magnitude M variable (Eq. 12) with parameter σ. The pdf of the log magnitude $L = \log M$ is then:

$$g(l) \;\stackrel{\text{def}}{=}\; \frac{e^{2l}}{\sigma^2} \; e^{-\frac{e^{2l}}{2\sigma^2}} \tag{26}$$

We are now trying to estimate the first moment of g: $\langle l \rangle_g \stackrel{\text{def}}{=} \int_{-\infty}^{+\infty} l \cdot g(l) \cdot dl$. An analytical expression is difficult to obtain, thus a numerical alternative is proposed below.

For any two parameter values σ and σ^*, and the associated pdfs $g(l)$ and $g^*(l)$, we can write:

$$\forall l \in \mathbb{R} \qquad g(l) \;=\; g^*\left(l - \log\frac{\sigma}{\sigma^*}\right) \tag{27}$$

therefore, the first moments of g and g^* are related as follows:

$$\langle l \rangle_g \quad = \quad \langle l \rangle_{g^*} \quad + \log \frac{\sigma}{\sigma^*} \tag{28}$$

Setting $\sigma^* = 1$, we obtain the first moment of g:

$$\langle l \rangle_g \quad = \quad \varepsilon \quad + \log \sigma \tag{29}$$

where ε is a constant equal to the geometric mean of Rayleigh-distributed data with parameter $\sigma^* = 1$.

Monte Carlo simulation leads to the numerical evaluation $\varepsilon \approx 0.06$. It is therefore reasonable to approximate σ with the geometric mean $e^{\langle l \rangle_g}$ of the Rayleigh distribution. Given the practical observation that speech only appears as a small tail to the right of the distribution of log-magnitudes L, it is then reasonable to approximate σ with *the geometric mean of all observed magnitude values*. In order to verify this in practice, we compared with the σ value produced by fitting the RSE model, as depicted in Fig. 11.

We note that the computational cost of this approximation is even smaller than that of RSE. In practice, with this approximation followed by USS, we systematically obtained ASR results close to, but slightly suboptimal to those of RSE-USS.

References

[1] J. Bitzer and K. U. Simmer, "Superdirective microphone arrays," in *Microphone Arrays*, M. Brandstein and D. Ward, Eds. Springer, 2001, ch. 2, pp. 19–38.

[2] R. Martin and C. Breithaupt, "Speech enhancement in the dft domain using Laplacian speech priors," in *Proc. of IWAENC 2003*, 2003.

[3] R. Gemello, F. Mana, and R. D. Mori, "A modified Ephraim-Malah noise suppression rule for automatic speech recognition," in *Proc. of ICASSP 2004*, 2004.

[4] H. Hermansky, N. Morgan, A. Bayya, and P. Kohn, "RASTA-PLP speech analysis technique," in *Proc. ICASSP'92*, 1992.

[5] S.Ikbal, H.Misra, and H.Bourlard, "Phase autocorrelation (PAC) derived robust speech features," in *Proc. ICASSP 2003*, 2003.

[6] A. P. Dempster, N. M. Laird, and D. B. Rubin, "Maximum likelihood from incomplete data via the EM algorithm," *Journal of the Royal Statistical Society, Series B*, vol. 39, pp. 1–38, 1977.

[7] "Speech processing, Transmission and Quality aspects (STQ); Distributed speech recognition; Advanced frond-end feature extraction algorithm; Compression algorithms," ETSI standard doc. ES 202 050 V1.1.4, November 2005.

[8] S. Boll, "Suppression of acoustic noise in speech using spectral subtraction," *IEEE Trans. on Acoustics, Speech and Signal Processing*, vol. 27, no. 2, April 1979.

[9] M. Berouti, R. Schwartz, and J. Makhoul, "Enhancement of speech corrupted by acoustic noise," in *Proc. ICASSP 79*, April 1979.

[10] C. Ris and S. Dupont, "Assessing local noise level estimation methods: application to noise robust asr," *Speech Communication*, vol. 34, pp. 141–158, 2001.

[11] G. Lathoud, M. Magimai.-Doss, B. Mesot, and H. Bourlard, "Unsupervised Spectral Subtraction for Noise-Robust ASR," in *Proc. the IEEE ASRU Workshop*, December 2005.

[12] R. Martin, "An efficient algorithm to estimate the instantaneous snr of speech signals," in *Proc. EUROSPEECH 1993*, 1993.

[13] H. Hermansky, "TRAP-TANDEM: Data-driven extraction of temporal features from speech," in *Proc. ASRU 2003*, 2003.

[14] H. Bourlard, S. Bengio, M. M. Doss, Q. Zhu, B. Mesot, and N. Morgan, "Towards using hierarchical posteriors for flexible automatic speech recognition systems," in *Proc. the DARPA EARS RT04 Workshop*, 2004.

[15] Y. Ephraim and D. Malah, "Speech enhancement using a minimum mean-square error short-time spectral amplitude estimator," in *Proc. ICASSP 1984*, 1984.

[16] J. Cohen, "Application of an auditory model to speech recognition," *Journal of the Acoustic Society of America*, vol. 85, no. 6, June 1989.

[17] D. V. Compernolle, "Noise adaptation in a hidden markov model speech recognition system," *Computer Speech and Language*, vol. 13, no. 1, 1989.

[18] C. M. Grinstead and J. L. Snell, *Introduction to Probability*. American Mathematical Society, 1997.

[19] B. Chen and P. Loizou, "Speech enhancement using a MMSE short time spectral amplitude estimator with Laplacian speech modeling," in *Proc. of ICASSP 2005*.

[20] G. Lathoud, M. Magimai.-Doss, and H. Bourlard, "Threshold selection for unsupervised detection, with an application to microphone arrays," in *Proc. ICASSP*, 2006.

[21] H. Hirsch and D. Pearce, "The Aurora experimental framework for the performance evaluation of speech recognition systems under noisy conditions," in *Proc. ISCA ITRW ASR2000*, September 2000.

[22] H. Hirsch and C. Ehrlicher, "Noise estimation techniques for robust speech recognition," in *Proc. ICASSP*, 1995.

[23] R. A. Cole, M. Fanty, M. Noel, and T. Lander, "Telephone speech corpus development at CSLU," 1994.

[24] G. Lathoud, M. Magimai.-Doss, and H. Bourlard, "Channel normalization for unsupervised spectral subtraction," IDIAP-RR 06-09, 2006.

[25] C. Avendano, S. Tibrewala, and H. Hermansky, "Multiresolution channel normalization for asr in reverberant environments," in *Proc. Eurospeech*, 1997.

[26] D. Gelbart and N. Morgan, "Evaluating long-term spectral subtraction for reverberant asr," in *Proc. the IEEE ASRU Workshop*, 2001.

[27] G. Lathoud, J.-M. Odobez, and D. Gatica-Perez, "AV16.3: an Audio-Visual Corpus for Speaker Localization and Tracking," in *Proc. the 2004 MLMI Workshop, S. Bengio and H. Bourlard Eds, Springer Verlag*, 2005.

[28] "Speech processing, Transmission and Quality aspects (STQ); Distributed speech recognition; Frond-end feature extraction algorithm; Compression algorithms," ETSI standard doc. ES 201 108 V1.1.2, April 2000.

[29] R. Leonard, "A database for speaker-independent digit recognition," in *Proc. ICASSP 2004*, 2004.

[30] J.-P. Delmas, *Introduction aux Probabilités*. Ellipses Marketing, 1993.